

MECHANISMS UNDERLYING TWO KINDS OF SURFACE EFFECTS ON ELASTIC CONSTANTS^{★★}

Yizhe Tang^{1,2*} Zhijun Zheng¹ Mengfen Xia^{1,3} Yilong Bai¹

(¹State Key Laboratory of Nonlinear Mechanics (LNM), Institute of Mechanics,
Chinese Academy of Sciences, Beijing 100190, China)

(²Graduate University of Chinese Academy of Sciences, Beijing 100049, China)

(³Department of Physics, Peking University, Beijing 100871, China)

Received 12 June 2009, revision received 15 September 2009

ABSTRACT Recently, people are confused with two opposite variations of elastic modulus with decreasing size of nano scale sample: elastic modulus either decreases or increases with decreasing sample size. In this paper, based on intermolecular potentials and a one dimensional model, we provide a unified understanding of the two opposite size effects. Firstly, we analyzed the microstructural variation near the surface of an fcc nanofilm based on the Lennard-Jones potential. It is found that the atomic lattice near the surface becomes looser in comparison with the bulk, indicating that atoms in the bulk are located at the balance of repulsive forces, resulting in the decrease of the elastic moduli with the decreasing thickness of the film accordingly. In addition, the decrease in moduli should be attributed to both the looser surface layer and smaller coordination number of surface atoms. Furthermore, it is found that both looser and tighter lattice near the surface can appear for a general pair potential and the governing mechanism should be attributed to the surplus of the nearest force to all other long range interactions in the pair potential. Surprisingly, the surplus can be simply expressed by a sum of the long range interactions and the sum being positive or negative determines the looser or tighter lattice near surface respectively. To justify this concept, we examined ZnO in terms of Buckingham potential with long range Coulomb interactions. It is found that compared to its bulk lattice, the ZnO lattice near the surface becomes tighter, indicating the atoms in the bulk located at the balance of attractive forces, owing to the long range Coulomb interaction. Correspondingly, the elastic modulus of one-dimensional ZnO chain increases with decreasing size. Finally, a kind of many-body potential for Cu was examined. In this case, the surface layer becomes tighter than the bulk and the modulus increases with decreasing size, owing to the long range repulsive pair interaction, as well as the cohesive many-body interaction caused by the electron redistribution.

KEY WORDS size effect, elastic modulus, surface effect, atomic/molecular potential, surface layer

I. INTRODUCTION

Recently, the rapid development of nanotechnologies and the extensive use of nano-scale materials and structures make the understanding and characterizing of their mechanical properties an urgent task. On the other hand, nano-scale materials and structures often exhibit very different from their

* Corresponding author. Tel.: +86-10-82543930; Fax: +86-10-82543977; E-mail: tangyz@lnm.imech.ac.cn

★★ Project supported by the National Natural Science Foundation of China (Nos. 10721202, 10432050, 10772012, 10732090) and the CAS innovation program (KJCX2-YW-M04).

conventional counterparts, even elastic moduli vary significantly when the sample size decreases to nano-scale.

Various experiments on nanofilms and nanowires show that the elastic moduli strongly depend on their size, i.e. their thickness or diameter. But, to the surprise of most people, the tendency of the variations are radically different for different materials^[1-4]. Atomic/molecular simulations also show the similar difference in the size-dependence. For instance, both molecular dynamics (MD) and molecular statics (MS) simulations of nanofilms based on Lennard-Jones potential^[5,6] show decreasing modulus with decreasing film thickness; Whereas MD simulations of ZnO nanowires based on Buckingham potential with long range Coulomb interactions^[7,8] show an inverse size effect, namely increasing modulus with decreasing nanowire diameter.

In fact, small size often leads to a large surface to volume ratio. Thus, the surface effects are usually considered to take the responsibility for the variations of mechanical properties at nano scale. Some theoretical models concerning surface effects, such as continuum models^[9-13] and microscopic models^[14-16] have been developed to explain the size dependence.

The two opposite size effects on elastic modulus implies that there might be different surface effects resulting from atomic/molecular interactions. For instance, Leach^[17] stated that ‘the surface properties of metals are such that the surface tends to relax inwards but systems described by two-body interactions tend to relax outwards’ in the popular book ‘Molecular Modelling’. Therefore, to identify the key aspects involved in atomic/molecular interactions governing the two opposite effects becomes a crucial issue in the study of mechanical properties of nano-scale materials. However, as far as we know, a unified understanding of these two different kinds of size and surface effects based on atomic/molecular interactions still remains open. As a matter of fact, the situation of these atoms or molecules near the surface is very different from those in the bulk in several aspects:

1. These atoms have smaller coordination number;
2. The atomic lattice near the surface is no longer the same as in the bulk, because the lattice near the surface has to be readjusted to achieve a new equilibrium, different from the bulk.

Obviously, the variations of elastic properties of nano-scale materials with decreasing size are merely a representation of these differences. Hence, from the viewpoint of the basic atomic/molecular interactions, the question is what is the unique atomic/molecular mechanism underlying the two different size effects on elastic properties.

In the present paper, the two kinds of surface effects on elastic modulus are studied based on atomic/molecular potentials. Firstly, the size effect of a fcc nanofilm with (001) surface on elastic moduli is discussed in terms of Lennard-Jones potential with long range attractive interaction. Then, the mechanism underlying the looser or tighter lattice near the surface is revealed. Furthermore, as a case study showing the inverse size effect, ZnO is examined by means of Buckingham potential with long range Coulomb interaction. Finally, many-body Finnis-Sinclair potential for Cu is examined to study the influence of many-body effect on the surface layer and size effects of elastic modulus.

II. SURFACE EFFECT ON ELASTIC MODULUS DUE TO LENNARD-JONES POTENTIAL

2.1. What is Surface Layer

Firstly, atoms on the free surface have smaller coordination number Z than its bulk, for example, for a cubic lattice $Z = 5$ on the surface rather than 6 in the bulk, see Fig.1.

The other important issue concerning the surface is the microstructural variation. In this section, as an example, we examine the microstructural variation near the surface in an fcc nanofilm, which has two {001} surface and $2N + 1$ (001) atomic layers in the thickness direction, i.e. [001] orientation, as shown in Fig.2(a). This nanofilm is originally constructed with the bulk lattice constant a and then readjusted to achieve a new equilibrium with two free surfaces.

Considering that the length/width to thickness ratio of the nanofilm is sufficiently high, we assume that:

- a) All atoms distribute uniformly in the length and width directions after the readjustment, neglecting the side boundary effect;
- b) All (001) plane atoms are still coplanar after the readjustment.

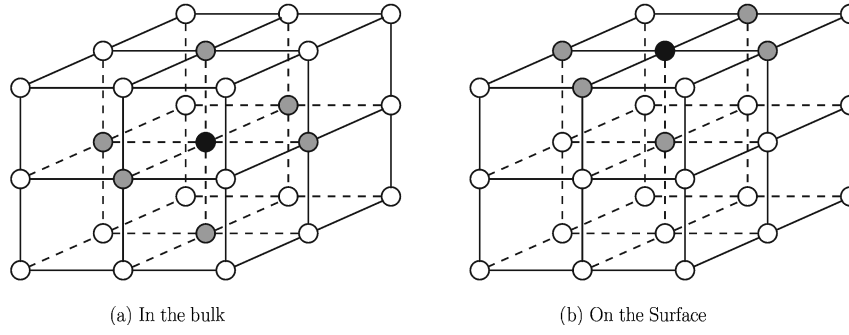


Fig. 1. Coordination number of atoms (black atoms).

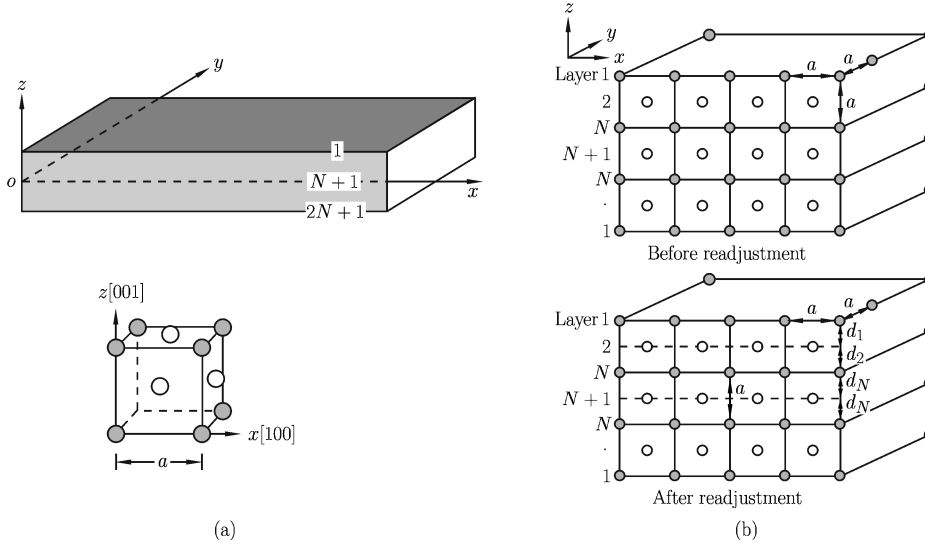


Fig. 2. (a) Sketch of the fcc nanofilm. (b) Variation of lattice after readjustment.

Hence, the only geometrical nonuniformity is the spacing of layers in the thickness direction. We denote the spacing between the i th and the $(i+1)$ th layer by d_i , $i=1, \dots, 2N$. After readjustment, the very interior lattice in a thick enough film should be uniform in all three directions and the corresponding lattice constant $2d_N$ should equal to a , as shown in Fig.2(b). The series of spacing d_i near surface can be determined by solving the force equilibrium equation of a representative atom of each layer in the thickness direction.

Lennard-Jones potential between atoms i and j is

$$u(r_{ij}) = 4\varepsilon_0 \left[\left(\frac{r_0}{r_{ij}} \right)^{12} - \left(\frac{r_0}{r_{ij}} \right)^6 \right] \quad (1)$$

which is used to describe the interactions between atoms, and the force between atoms i and j can be written as

$$\mathbf{f}(\mathbf{r}_{ij}) = 48 \left(\frac{\varepsilon_0}{r_0} \right) \left[\left(\frac{r_0}{r_{ij}} \right)^{13} - \frac{1}{2} \left(\frac{r_0}{r_{ij}} \right)^7 \right] \frac{\mathbf{r}_{ij}}{r_{ij}} \quad (2)$$

So, the z -component of the force can be written as

$$f_z(r_{ij}) = 48z_{ij} \left(\frac{\varepsilon_0}{r_0^2} \right) \left[\left(\frac{r_0}{r_{ij}} \right)^{14} - \frac{1}{2} \left(\frac{r_0}{r_{ij}} \right)^8 \right] \quad (3)$$

and the total z -component force acting on a representative atom in the i th layer can be written as

$$F_z^i = \sum_{r_{ij} \leq r_c} f_z(r_{ij}) = 0 \quad (i = 1, \dots, 2N+1) \quad (4)$$

where \mathbf{r}_{ij} is the vectorial distance between atoms i and j , $\mathbf{r}_{ij} = \mathbf{r}_i - \mathbf{r}_j$, r_{ij} is the modulo of \mathbf{r}_{ij} ; x_{ij} , y_{ij} and z_{ij} are the corresponding coordinate components of \mathbf{r}_{ij} , respectively, ε_0 and r_0 are the two potential parameters and r_c is the cutoff radius.

Considering that the long range attractive interaction in Eq.(3) is proportional to r_{ij}^{-7} , then the cutoff radius of $r_c = 8r_{\text{nearest}}$ is chosen to guarantee a precision better than a millionth in calculation, where $r_{\text{nearest}} = 2^{1/6}r_0$ is the distance corresponding to the minimum of Lennard-Jones potential, since $r_c^{-7}/r_{\text{nearest}}^{-7} = 8^{-7} = 4.8 \times 10^{-7}$ when $r_c/r_{\text{nearest}} = 8$.

Because the x - o - y plane is symmetric, there are N independent equations in Eq.(4) for the thin film. By solving these equations simultaneously with iterative method, the spacing series d_i can be obtained. The results for the cases $N = 3, 6$ and 20 and the corresponding curve fitting are shown in Table 1 and Fig.3 respectively. There is a slight difference between the cases of $N = 3, 6$ and 20 , as shown in Table 1, and $d_8 \approx d_9 \approx d_{10}$, for the case $N = 20$. The lattice constant in the bulk $2d_{20} = 0.97158 \cdot 2^{2/3} r_0$ also agrees well with the lattice constant for infinite fcc lattice $a = 0.971 \cdot 2^{2/3} r_0$ given by Kittel^[18].

Table 1. Spacing series d_i : (a) $N = 3$; (b) $N = 6$; (c) $N = 20$

Spacing ($2^{2/3}r_0$)	(a) $N=3$	(b) $N=6$	(c) $N=20$
d_1	0.498041	0.498021	0.498021
d_2	0.488467	0.488392	0.488392
d_3	0.486774	0.486535	0.486535
d_4	-	0.486029	0.486030
d_5	-	0.485866	0.485865
d_6	-	0.485814	0.485810
d_7	-	-	0.485793
d_8	-	-	0.485790
d_9	-	-	0.485790
d_{10}	-	-	0.485790
	-	-	...

It can be seen from Fig.3 that the spacing near the surface is a little longer than that in the bulk, and this deviation decreases rapidly. d_5 is only 0.011% greater than d_6 , for the case $N = 20$. So, the non-uniform region is a very thin layer (8 atomic layers at most) near the surface, named as the surface layer later.

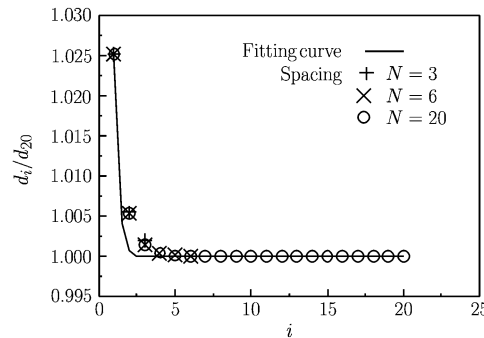


Fig. 3. Spacings of two neighboring layers normalized by d_{20} , for $N = 3, 6$ and 20 .

To quantitatively assess the thickness of the surface layer, the data is fitted with an exponential formula $d_i/d_N = 1 + e^{-i/t_0}$, and $t_0 = 0.27232$ for $N = 20$. This means that a reduction of $1/e$ in spacing d appears when the layer's number increases to t_0 .

From all the above discussions, the special features of the surface are: the nonuniform lattice and smaller coordination numbers of the atoms near the surface.

2.2. Effect of Surface Layer on Elastic Modulus

2.2.1. Effect of coordination number of surface layer on elastic modulus

In this sub-section we discuss the effect of the coordination number of surface layer on elastic modulus in terms of a simple model. Generally speaking, the total energy U can be written as the sum of two parts: the bulk term and the non-bulk term:

$$U = \frac{1}{2} \sum_i \sum_{j \neq i} u(r_{ij}) = \frac{1}{2} \sum_{i \in \text{bulk}} \sum_{j \neq i} u(r_{ij}) + \frac{1}{2} \sum_{i \notin \text{bulk}} \sum_{j \neq i} u(r_{ij}) \quad (5)$$

where $u(r_{ij})$ is the pair potential between atoms i and j . The bulk term consists of the energy of all equivalent atoms and the rest is the non-bulk term, see Fig.4. Clearly, the bulk term is independent of sample size, while the non-bulk term may be size-dependent.

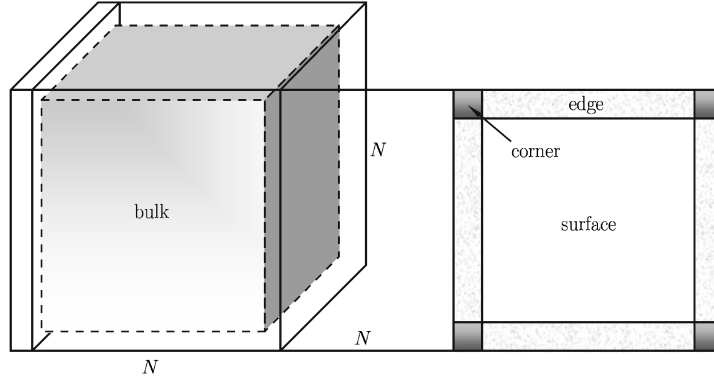


Fig. 4. Schematic diagram of a finite cubic crystalline lattice showing four different parts. The atoms in the bulk, surface, edge and corner have different coordination numbers.

For example, as shown in Fig.4, for a finite cubic crystalline lattice containing $M = N^3$ atoms, after taking only the nearest neighboring interaction into account, we can write the total energy of the cubic lattice as

$$U = \frac{u(r)}{2} \left\{ Z_1 (N-2)^3 + Z_2 \left[6(N-2)^2 \right] + Z_3 [12(N-2)] + 8Z_4 \right\} \quad (6)$$

where N is the total of the layers in each directions, Z_1 , Z_2 , Z_3 , and Z_4 are the coordination numbers of each atom in the bulk, surface, edge and corner respectively, r is the distance between two nearest atoms and should be a function of strain. The term with preceding factor Z_1 in Eq.(6) is the bulk term, and the rest are non-bulk terms. The strain energy density of the cubic lattice W can be written as

$$W = (U - U_0) / V \quad (7)$$

where U_0 is the total energy of the cubic lattice without any deformation, $V = (Nr)^3$ is the volume of the cubic lattice as conventionally defined^[6]. Also, stresses σ_x , σ_y and σ_z can be written as

$$\sigma_x = \frac{\partial W}{\partial \varepsilon_x}, \quad \sigma_y = \frac{\partial W}{\partial \varepsilon_y}, \quad \sigma_z = \frac{\partial W}{\partial \varepsilon_z} \quad (8a)$$

Now let us consider the contribution of the non-bulk terms on the elastic bulk modulus K as an example. Suppose $\varepsilon_x = \varepsilon_y = \varepsilon_z = \varepsilon$, then volumetric strain $e = \varepsilon_x + \varepsilon_y + \varepsilon_z = 3\varepsilon$, hydrostatic stress $\Theta = (\sigma_x + \sigma_y + \sigma_z)/3$ can be written as

$$\Theta = \frac{\partial W}{\partial e} = \frac{1}{3} \frac{\partial W}{\partial \varepsilon} \quad (8b)$$

The bulk modulus K is defined as

$$K = \frac{\partial^2 W}{\partial e^2} = \frac{1}{9} \frac{\partial^2 W}{\partial \varepsilon^2} = \frac{1}{18N^3r^3} \frac{\partial^2 u(r)}{\partial \varepsilon^2} \left\{ Z_1 (N-2)^3 + Z_2 \left[6(N-2)^2 \right] + Z_3 [12(N-2)] + 8Z_4 \right\} \quad (9)$$

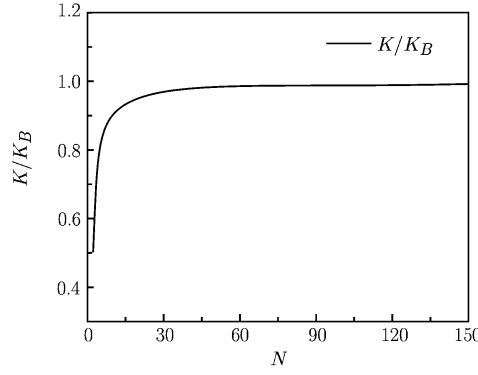


Fig. 5. Normalized bulk modulus K/K_B as a function of N .

Obviously, K is a function of N , i.e. size-dependent. Only if $Z_1 = Z_2 = Z_3 = Z_4$, K tends to be $(Z_1 \partial^2 u(r)) / (18r^3 \partial \varepsilon^2)$, namely the size-independent value of the bulk material K_B . However, for a cubic lattice $Z_1 = 6$, $Z_2 = 5$, $Z_3 = 4$, and $Z_4 = 3$, namely $Z_{2,3,4} < Z_1$, the modulus K is less than its bulk value K_B with decreasing size, see Fig.5. Clearly, the difference in coordination numbers between the non-bulk and the bulk atoms results in a size effect on elastic modulus, regardless of any variation of lattice spacing near the surface.

2.2.2. Effect of nonuniform spacing of surface layer on elastic modulus

Although smaller coordination numbers of surface atoms can induce size effect on elastic modulus, as mentioned in previous section, the variation of lattice spacing near the surface results in even more significant size effect on elastic properties. Now, as a concrete case study, we turn to discuss the elastic moduli of a fcc nanofilm with such a surface. As shown in Fig.3 and Table 1, we suppose that the spacing between all layers except the outmost six layers (near the upper and lower surface) are uniform along the thickness direction (with uniform lattice constant $a = 2d_N$, $N = 20$). Also, the nanofilm is assumed to have uniform strains ε_x , ε_y and ε_z in three directions. Then the stresses σ_x , σ_y and σ_z can be obtained by dividing the corresponding forces by the cross section areas. The last but not least point is that we take the second and third nearest neighbors' effects into account. The significance of the issue is explained in §III.

The force between two atoms i and j can be expanded as a function of strains

$$\mathbf{f}(\mathbf{r}_{ij} + \Delta \mathbf{r}_{ij}) = f(|\mathbf{r}_{ij} + \Delta \mathbf{r}_{ij}|) \frac{\mathbf{r}_{ij} + \Delta \mathbf{r}_{ij}}{|\mathbf{r}_{ij} + \Delta \mathbf{r}_{ij}|} \approx \left[f(\mathbf{r}_{ij}) + \frac{\partial f(\mathbf{r}_{ij})}{\partial r_{ij}} \Delta r_{ij} \right] \frac{\mathbf{r}_{ij}}{r_{ij}} \quad (10)$$

where \mathbf{r}_{ij} is the vectorial distance between atoms i and j , r_{ij} is the modulo of \mathbf{r}_{ij} , and

$$\begin{aligned} \Delta r_{ij} &= |\mathbf{r}_{ij} + \Delta \mathbf{r}_{ij}| - r_{ij} \\ &= \left[x_{ij}^2 (1 + \varepsilon_x)^2 + y_{ij}^2 (1 + \varepsilon_y)^2 + z_{ij}^2 (1 + \varepsilon_z)^2 \right]^{1/2} - (x_{ij}^2 + y_{ij}^2 + z_{ij}^2)^{1/2} \\ &\approx \frac{x_{ij}^2 \varepsilon_x + y_{ij}^2 \varepsilon_y + z_{ij}^2 \varepsilon_z}{r_{ij}} \end{aligned} \quad (11)$$

The x -component of the force can be written as

$$f_x(\mathbf{r}_{ij} + \Delta \mathbf{r}_{ij}) \approx \left[f(\mathbf{r}_{ij}) + \frac{\partial f(\mathbf{r}_{ij})}{\partial r_{ij}} \Delta r_{ij} \right] \frac{x_{ij}}{r_{ij}}. \quad (12)$$

While calculating σ_x , we cut the nanofilm into two equal parts, see Fig.6(a). The total normal forces exerted on the right part by the left can be written as

$$F_x = \sum_{i=1}^{2N+1} m F_x^i = 2 \sum_{i=1}^6 m F_x^i + (2N + 1 - 12) m F_x^{\text{inner}} \quad (13)$$

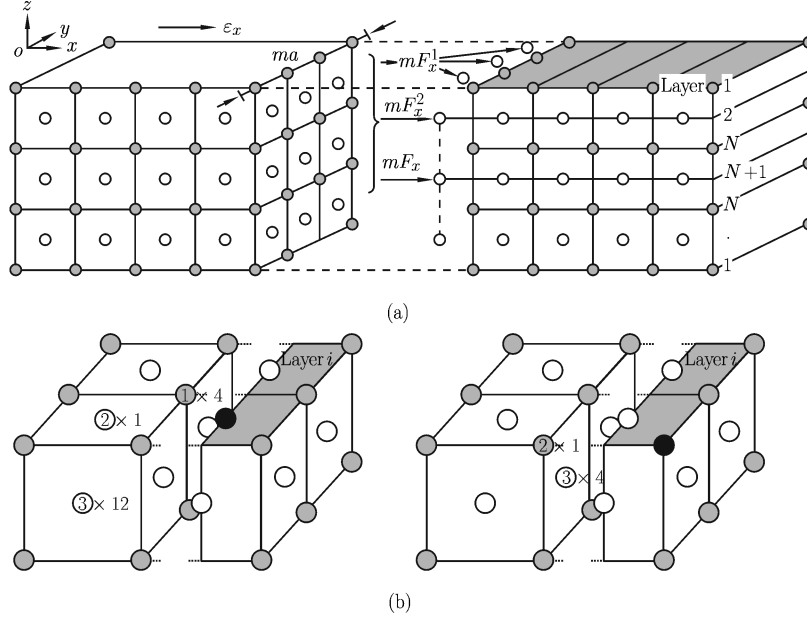


Fig. 6. Schematic diagram for force calculation: (a) forces exerted on the first, second, \dots , $(N + 1)$ th layers of the right half part from the left. (b) the first (①), second (②) and third (③) nearest neighbor atoms of a pair of representative atoms (black) in the i th layer for the calculation of the total forces exerted on the pair of representative atoms.

where m is the total number of unit cells in the two directions in plane, F_x^i is the total forces exerted on a pair of representative atoms (two black atoms in Fig.6(b)) in the i th layer of the right half part by the whole left half part. F_x^i can be written as

$$F_x^i = \sum_{\substack{r_{ij} < r_{3rd} \\ j \in \text{left part}}} f_x(r_{ij} + \Delta r_{ij}) \quad (14)$$

where r_{3rd} is the distances between an bulk atom and its third nearest neighbor, i.e. the cutoff distance. Whereas, $F_x^{\text{inner}} = F_x^{N+1}$, is the total force exerted on a pair of representative atoms in the $(N + 1)$ th layer, as shown in Fig.6(a). So, the second item on the right hand side of Eq.(13) means that all layers except the outmost six layers near the surface are uniform.

The area of (100) cross section can be written as

$$S_x = ma \left[\frac{a}{2} (2N + 1 - 12) + 2 \sum_{i=1}^6 d_i \right] \quad (15)$$

Therefore, the normal stress σ_x and σ_y can be written as

$$\sigma_x = \frac{F_x}{S_x} \quad (16)$$

$$\sigma_y = \frac{F_y}{S_y} \quad (17)$$

where $S_y = S_x$.

In order to calculate σ_z , we have to cut the nanofilm into two parts from the middle of the nanofilm (between the N th layer and the $(N + 1)$ th layer). Because of the uniformity of the bulk lattice, the total normal force exerted on one part by the other can be written as

$$F_z = \sum_{i=1}^{2m} mF_z^i = 2m^2 F_z^{\text{inner}} \quad (18)$$

where $F_z^{\text{inner}} = F_z^{N+1}$. Again, σ_z can be written as

$$\sigma_z = \frac{F_z}{S_z} \quad (19)$$

where $S_z = (ma)^2$ is the area of (001) cross section. σ_x , σ_y and σ_z are linear functions of ε_x , ε_y and ε_z . Substituting Eqs.(12) ~ (15) and (18) into Eqs.(16), (17) and (19) yields the elasticity relations

$$\begin{aligned} \sigma_x &= C_{11}\varepsilon_x + C_{12}\varepsilon_y + C_{13}\varepsilon_z \\ \sigma_y &= C_{21}\varepsilon_x + C_{22}\varepsilon_y + C_{23}\varepsilon_z \\ \sigma_z &= C_{31}\varepsilon_x + C_{32}\varepsilon_y + C_{33}\varepsilon_z \end{aligned} \quad (20)$$

where the elastic constants C_{ij} are given by

$$\begin{aligned} C_{11} &= \frac{a}{S_x} \left[(2N - 12 + 1)(c_1 + 2c_2 + 6c_3) - 2 \left(\frac{1}{4}c_1 + 3c_3 \right) + 6c_1 + 24c_2 \right. \\ &\quad \left. + \frac{a^2}{2} \sum_{i=1}^6 \frac{c_{1\text{st}}^i}{(r_{1\text{st}}^i)^2} + 17a^2 \sum_{i=1}^6 \frac{c_{3\text{rd}}^i}{(r_{3\text{rd}}^i)^2} + a^2 \sum_{i=1}^6 \frac{c_{1\text{3rd}}^i}{(r_{1\text{3rd}}^i)^2} \right] \\ C_{12} &= \frac{a}{S_x} \left[(2N - 12 + 1) \left(\frac{1}{2}c_1 + 3c_3 \right) - 3c_3 + 6c_1 \right. \\ &\quad \left. + 24c_2 + 8a^2 \sum_{i=1}^6 \frac{c_{3\text{rd}}^i}{(r_{3\text{rd}}^i)^2} + a^2 \sum_{i=1}^6 \frac{c_{1\text{3rd}}^i}{(r_{1\text{3rd}}^i)^2} \right] \\ C_{13} &= \frac{a}{S_x} \left[(2N - 12 + 1) \left(\frac{1}{2}c_1 + 3c_3 \right) - 2 \left(\frac{1}{4}c_1 + \frac{3}{2}c_3 \right) \right. \\ &\quad \left. + 2 \sum_{i=1}^6 \frac{d_i^2 c_{1\text{st}}^i}{(r_{1\text{st}}^i)^2} + 20 \sum_{i=1}^6 \frac{d_i^2 c_{3\text{rd}}^i}{(r_{3\text{rd}}^i)^2} + 4 \sum_{i=1}^6 \frac{(d_i + d_{i+1})^2 c_{1\text{3rd}}^i}{(r_{1\text{3rd}}^i)^2} \right] \\ C_{21} &= C_{12}, \quad C_{22} = C_{11}, \quad C_{23} = C_{13}, \quad C_{31} = \frac{c_1 + 6c_3}{a}, \quad C_{32} = C_{31}, \quad C_{33} = \frac{2(c_1 + 2c_2 + 6c_3)}{a} \end{aligned} \quad (21)$$

where $r_{1\text{st}}$, $r_{2\text{nd}}$ and $r_{3\text{rd}}$ are distances between an bulk atom and its first, second and third nearest neighbor atoms, $r_{1\text{st}}^i$, $r_{2\text{nd}}^i$, $r_{3\text{rd}}^i$ and $r_{1\text{3rd}}^i$ with superscript i are distances between an arbitrary representative atom in the i th layer and its first, second and third nearest neighbor atoms (there are two different kinds of third nearest neighbor atoms, $r_{3\text{rd}}^i$ and $r_{1\text{3rd}}^i$ are the corresponding distances). c_1 , c_2 , c_3 , $c_{1\text{st}}^i$, $c_{2\text{nd}}^i$, $c_{3\text{rd}}^i$ and $c_{1\text{3rd}}^i$ are the corresponding stiffness, for example,

$$c_1 = - \frac{\partial f(r_{ij})}{\partial r_{ij}} \Big|_{r_{ij}=r_{1\text{st}}} \quad \text{and} \quad c_{1\text{st}}^1 = - \frac{\partial f(r_{ij})}{\partial r_{ij}} \Big|_{r_{ij}=r_{1\text{st}}^1}$$

To illustrate the meaning of the stiffness, considering the looser surface discussed in §2.1, The stiffness near the surface $c_{1\text{st}}^1 = 19.88 (4\varepsilon_0/r_0^2)$ is less than its bulk value $c_1 = 25.36 (4\varepsilon_0/r_0^2)$, because $d_1 > d_{20}$, see Table 1.

All elastic constants except C_{31} , C_{32} and C_{33} depend on N . For the case of $\sigma_y = \sigma_z = 0$, according to $\sigma_x = E\varepsilon_x$, the elastic modulus E in $\langle 100 \rangle$ direction can be written as

$$E = \frac{(C_{11} - C_{12})(C_{12}C_{33} - 2C_{31}C_{13} + C_{11}C_{33})}{C_{11}C_{33} - C_{31}C_{13}} \quad (22)$$

The obtained relation between E/E_∞ and N is shown in Fig.7, where E_∞ is the corresponding bulk value as N approaches to infinite, i.e. $E_\infty = \lim_{N \rightarrow \infty} E(N)$. It is found that the elastic modulus in $\langle 100 \rangle$ decreases with decreasing N .

To justify the above analysis, the elastic moduli E in $\langle 100 \rangle$ direction for different thickness, $N = 6$, 15 and 30, are also numerically calculated using molecular statics (MS). The corresponding simulations have $53 \times 67 \times 13$, $53 \times 67 \times 31$ and $65 \times 67 \times 61$ layers in three directions, respectively. For each given thickness, the test piece is firstly relaxed for energy minimum, and then stretched in $\langle 100 \rangle$ direction by

strain step of 0.1% to 1%. At each strain step, the test piece is relaxed to the energy minimum, and then the corresponding normal stress in $\langle 100 \rangle$ direction is calculated. The elastic moduli E in $\langle 100 \rangle$ direction is obtained by linear fitting of $\sigma_x \sim \varepsilon_x$. The modulus for different thickness obtained with MS simulations is also shown in Fig.7. It can be seen from Fig.7 that the result of Eq.(22) agrees well with the result of molecular statics.

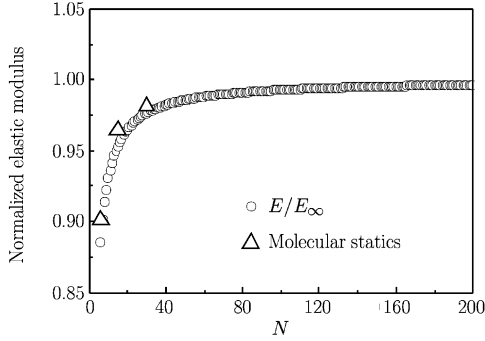


Fig. 7. Normalized elastic moduli E in $\langle 100 \rangle$ direction as functions of N obtained by MS simulation (open triangles) and Eq.(22) (open circles).

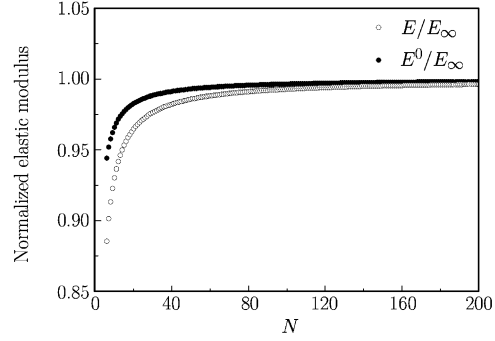


Fig. 8. Comparison of the variations of normalized elastic modulus in $\langle 100 \rangle$ direction as a function of N with uniform (●) and looser (○) surface layers.

In order to split the effect of the smaller coordination number on the surface from that of the looser surface lattice on elastic modulus, we also examined a virtual uniform nanofilm with d_N ($N = 20$) as its spacing in three axial directions. The corresponding expressions of the elastic constants C_{ij}^0 and modulus in $\langle 100 \rangle$ direction E^0 are

$$\begin{aligned} C_{11}^0 &= \frac{2}{(2N+1)a} [(2N+1-4)(c_1+2c_2+6c_3) + 2(1.75c_1+4c_2+6c_3)] \\ C_{12}^0 &= \frac{2}{(2N+1)a} [(2N+1-4)(0.5c_1+3c_3) + 2(c_1+3c_3)] \\ C_{13}^0 &= \frac{2}{(2N+1)a} [(2N+1-4)(0.5c_1+3c_3) + 2(0.75c_1+3c_3)] \end{aligned} \quad (23)$$

$$\begin{aligned} C_{21}^0 &= C_{12}^0, \quad C_{22}^0 = C_{11}^0, \quad C_{23}^0 = C_{13}^0, \quad C_{31}^0 = \frac{c_1+6c_3}{a}, \quad C_{32}^0 = C_{31}^0 \\ C_{33}^0 &= \frac{2(c_1+2c_2+6c_3)}{a} \\ E^0 &= \frac{(C_{11}^0 - C_{12}^0)(C_{12}^0 C_{33}^0 - 2C_{31}^0 C_{13}^0 + C_{11}^0 C_{33}^0)}{C_{11}^0 C_{33}^0 - C_{31}^0 C_{13}^0} \end{aligned} \quad (24)$$

The normalized modulus E^0/E_∞ in $\langle 100 \rangle$ direction is shown in Fig.8, showing the decreases with decreasing thickness, owing to the smaller coordination number on the surface. This effect is also seen in simple cubic lattice^[16].

For comparison, we put the two curves of E/E_∞ and E^0/E_∞ together in Fig.8. Now, we can conclude that although both smaller coordination number and looser surface layer contribute to the reduction of the elastic moduli, the looseness of surface layer reduces the modulus more pronouncedly. The reduction of elastic modulus in $\langle 100 \rangle$ direction is about 11% when $N = 6$ and 1% only when $N = 60$ (about several nanometers thick). This tendency agrees well with other numerical results^[6]. In Ref.[6], the reduction of elastic modulus in $\langle 100 \rangle$ direction is about 10%, for the film with 13 layers of atoms.

III. MECHANISMS UNDERLYING ATOMIC SPACING NEAR SURFACE

Now, we ask why the surface layer with L-J potential becomes looser and whether the looser surface is universal or not. Apparently, when we separate an infinite bulk medium into two semi-infinite bodies, a new planar surface is created. Accordingly, the atomic lattice near the surface is differentiated from

the original uniform bulk lattice, either expanding outwards owing to the repulsive forces or shrinking inwards owing to the attractive forces, resulting from all inside atoms of the semi-infinite body. To illustrate the surface state clearly, let us examine a long one-dimensional chain of $N + 1$ atoms with spacing a , as shown in Fig.9.

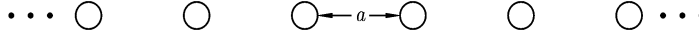


Fig. 9. Sketch of a long one-dimensional atomic chain.

After adopting a pair potential $u(r_{ij})$ and taking the superposition of energy for the atomic system, where r_{ij} is the distance between atoms i and j , the total potential energy of the atomic chain can be written as

$$u_{\text{tot}} = \frac{1}{2} \sum_{i=1}^{N+1} \sum_{j \neq i}^{N+1} u(r_{ij}) \approx \frac{1}{2} (N+1) 2 \sum_{n=1}^{N/2} u(na) \quad (25)$$

In the latter approximation works, provided the chain is such long that the ends of the chain are neglected and all atoms could be considered as identical ($N \gg 1$), or the chain is a large circle.

Now, we can determine the equilibrium lattice constant a_0 , by means of the minimization of the total potential energy with respect to the lattice spacing a :

$$\frac{du_{\text{tot}}}{da} \approx (N+1) \sum_{n=1}^{N/2} n \frac{\partial u(x)}{\partial x} \Big|_{x=na_0} = (N+1) \sum_{n=1}^{N/2} nu'(na_0) = 0 \quad (26)$$

where $u'(x)$ denotes the derivative of function u with respect to its argument x . Since the total of atoms $N + 1$ is a constant, the equilibrium lattice constant a_0 should satisfy the following condition,

$$\sum_{n=1}^{N/2} nu'(na_0) = 0 \quad (27a)$$

Additionally, from this equilibrium condition, the nearest force $-u'(a_0)$ (positive indicating repulsive force as usually defined) at equilibrium state can be expressed by a certain sum of longer range interactions ($n \geq 2$) as

$$-u'(a_0) = \sum_{n=2}^{N/2} nu'(na_0) \quad (27b)$$

Since the terms $u'(na_0)$ with $n \geq 2$ rather than $-u'(na_0)$ appear frequently later, we name them as longer interactions. Clearly, $u'(na_0) > 0$ or < 0 represents attractive or repulsive interactions, respectively. On the other hand, for the one-dimensional case, the one-side force acting on a representative atom i from all unilateral atoms (for instance all $N/2$ atoms left to the representative atom i , see the shaded area in Fig.10) can be written as

$$\mathbf{f}_i = - \sum_{j=i+1}^{i+N/2} \frac{\partial u(r_{ij})}{\partial \mathbf{r}_i} = - \sum_{j=i+1}^{i+N/2} \frac{\partial u(r_i - r_j)}{\partial \mathbf{r}_i} \mathbf{e}_r \quad (28a)$$

where \mathbf{e}_r is the unit vector of the position vector \mathbf{r} . Note that positive \mathbf{f}_i denotes the repulsive force acting on atom i from all atoms in the left semi-infinite chain, and vice versa. Since $\mathbf{r}_{ij} = \mathbf{r}_i - \mathbf{r}_j$ can

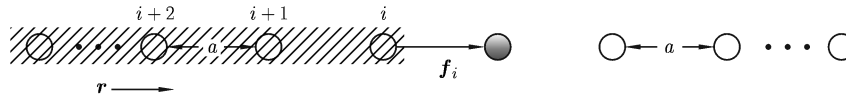


Fig. 10. One-side force acting on atom i .

be rewritten as na in one-dimensional chain, the one-side force \mathbf{f}_i acting on the representative atom i in the bulk with uniform lattice spacing a_0 can be written as

$$\mathbf{f}_i = - \sum_{n=1}^{N/2} u'(na_0) \mathbf{e}_r = -u'(a_0) \mathbf{e}_r - \sum_{n=2}^{N/2} u'(na_0) \mathbf{e}_r \quad (28b)$$

Equation (28b) implies that the one-side force from the left semi-infinite body acting on the representative atom in the bulk is governed by the surplus of the nearest force $-u'(a_0)$ to all other long range interactions $u'(na_0)$ in a pair potential. After substituting the equilibrium condition Eq.(27b) into the one-side force expression in Eq.(28b), one can obtain an alternative expression of the one-side force from the left semi-infinite body acting on the representative atom in the bulk as

$$\mathbf{f}_i = \sum_{n=2}^{N/2} (n-1) u'(na_0) \mathbf{e}_r \quad (29)$$

This means that the one-side force from semi-infinite chain acting on a representative atom in the bulk can be expressed exclusively by a certain sum of the long range atomic/molecular interactions of a pair potential from $n \geq 2$. More specifically, provided all derivatives $u'(na_0) > 0$ for $(n \geq 2)$, i.e. all $n \geq 2$ atoms are in the range of attraction-dominated pair interaction, the one-side force from semi-infinite chain acting on a representative atom in the bulk would be positive, namely a repulsive force. At first glance, this result seems to be very peculiar and abnormal. As a matter of fact, the repulsive one-side force is resulting from the surplus of the force due to the nearest atom ($n = 1$),

namely $-u'(a_0) = \sum_{n=2}^{N/2} nu'(na_0)$, to the long-range interactions from all other atoms ($n \geq 2$), namely $\sum_{n=2}^{N/2} u'(na_0)$. In addition, it should be noted that the above simple result (Eq.(29)) is obtained in terms of one-dimensional chain model, hence with no relation with the details of lattice. Provided an equivalent one-dimensional lattice model containing information about the lattice structure and orientation is adopted, the result depends not only on the potential but also the lattice structure and orientation, however the expression is not going to be so concise.

Now, we take Lennard-Jones potential as an example. It is well known that Lennard-Jones potential is a kind of potential with long range attractive interactions, the unilateral force f_i acting on an atom in the bulk should be repulsive according to Eq.(29). The value of the force f_i in one dimensional chain is accordingly calculated to be $0.02417 (4\varepsilon_0/r_0)$, which means a repulsive force. For the case of an infinite uniform fcc lattice being separated into two semi-infinite bodies by a (001) plane, the one-side force exerting on a representative atom i from all unilateral atoms (for instance all atoms above atom i , as shown in Fig.11) can also be calculated in a similar way and it is $0.6841 (4\varepsilon_0/r_0)$, also repulsive force but much greater than that of the one dimensional chain. Consequently, the lattice near the free surface for a fcc lattice with Lennard-Jones potential would be looser than the bulk.

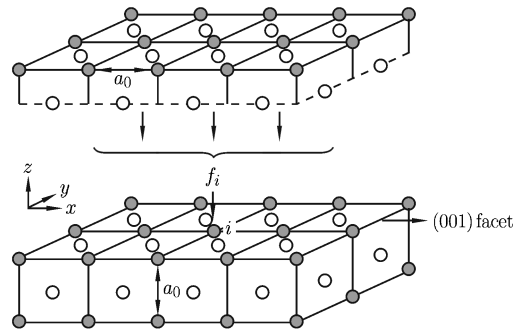


Fig. 11. Schematic diagram of one-side force exerted on atom i from all unilateral atoms above (001) facet.

More generally speaking, since the one-side force from a semi-infinite body acting on a representative atom in the bulk, Eq.(29), is determined by the summation of long range interactions starting from

$n = 2$, any predominant attractive long range pair interaction $u'(na) > 0$ for $n \geq 2$, should also lead to a repulsive one-side force. As a matter of fact, all Mie-type potentials

$$u(r) = \varepsilon_0 \left[\frac{k}{l-k} \left(\frac{r_0}{r} \right)^l - \frac{l}{l-k} \left(\frac{r_0}{r} \right)^k \right] \quad (30)$$

where ε_0 is the energy when distance $r = r_0$, l and k are the power indices of repulsive and attractive interactions respectively and $l > k$, see Fig.12(a). Figure 12(a) shows this kind of long range attractive interactions and demonstrates repulsive one-side force in the bulk. Whilst, an attractive one-side force would need some predominant repulsive long range interaction, namely predominantly $u'(na) < 0$. This implies a tendency of increasing potential with decreasing distance between two atoms and this would be against the existence of a minimum energy in the pair potential, necessary for a stable equilibrium state. To balance the two tendencies, such potentials showing attractive one-side force in the bulk should present a certain minimum relevant to the equilibrium state $a = a_0$ as well as a maximum to guarantee the existence of predominant repulsive long range interactions $u'(na) < 0$, as shown in Fig.12(b). However, which potentials in reality could present such a feature? Because of the importance of this matter in the surface effect, we discuss this issue in details in §IV.

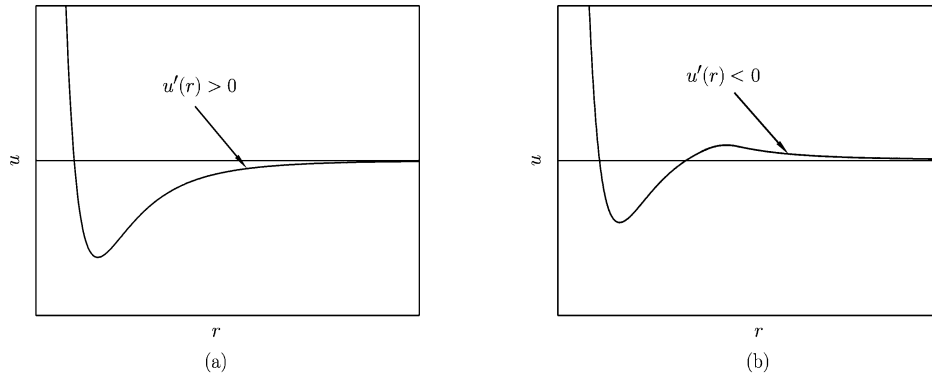


Fig. 12. Two kinds of potential energy profiles, the predominant long range interaction is: (a) attractive interaction, and (b) repulsive interaction.

IV. SURFACE EFFECT ON ELASTIC MODULUS DUE TO BUCKINGHAM POTENTIAL WITH COULOMB INTERACTION

In this section, we examine a kind of potential including long range repulsive interaction, namely Buckingham potential with Coulomb interaction, to study the influence of long range repulsive interactions on the microstructure of the surface layer of ZnO. The form of this potential is written as

$$u(r_{ij}) = \frac{q_i q_j}{r_{ij}} + A \exp \left(\frac{-r_{ij}}{\rho} \right) - \frac{C}{r_{ij}^6} \quad (31)$$

where r_{ij} is the distance between two ions; q_i is the charge of ion i ; A , ρ and C are potential parameters and their values for ZnO are listed in Table 2. The first term in Eq.(31) represents the long range Coulomb interaction.

Table 2. Short range interaction parameters for zinc oxide, from Ref.[7]

	A (eV)	ρ (Å)	C (eV Å ⁶)
O ²⁻ O ²⁻	9547.96	0.21916	32.0
Zn ²⁺ O ²⁻	527.70	0.35810	0.0
Zn ²⁺ Zn ²⁺	0	0	0



Fig. 13. Sketch of one-dimensional ZnO chain.

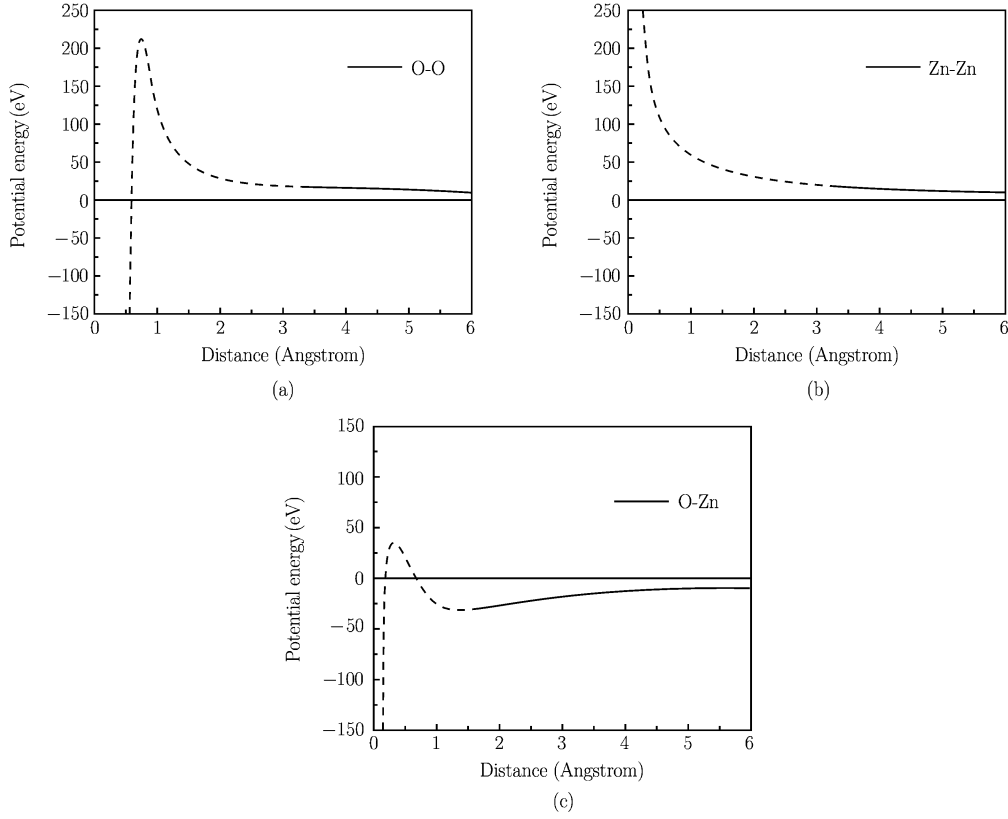


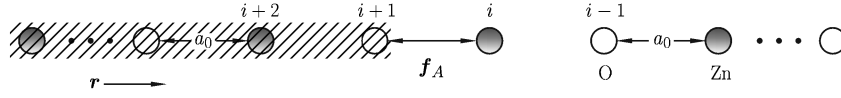
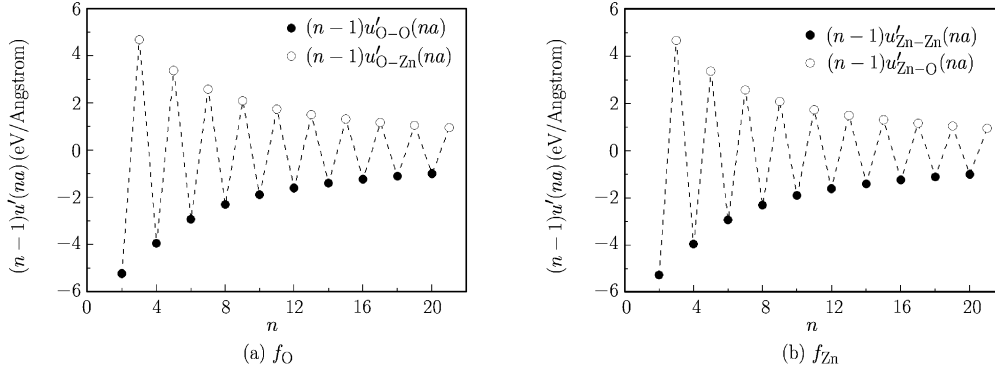
Fig. 14. Profile of pair potential for: (a) O-O; (b) Zn-Zn; (c) O-Zn.

As discussed in §III, we examine an infinite one-dimensional ZnO chain, as shown in Fig.13. For such a binary compound, three pair potentials: $u_{\text{O-O}}$, $u_{\text{Zn-Zn}}$ and $u_{\text{O-Zn}}$ should be considered. The profiles of these three pair potentials are shown in Fig.14. In addition, since the chain presents a lattice with period $2a$, see Fig.13, the first two potentials for the atoms belonging to the same specie are valid only for the atoms with period $n \times 2a$, see solid lines in Fig.14(a) and Fig.14(b), namely with its second near atom and so on; whereas the last potential for two different atoms is valid to every atom with its nearest atom and other atoms with period $2a$ thereafter, see the solid line in Fig.14(c). So, the total potential of the chain, as in Eq.(25), can be expressed by,

$$\begin{aligned}
 u_{\text{tot}} &\approx \frac{N}{2} 2 \{ u_{A-B}(a) + u_{A-B}(3a) + \dots + u_{A-A}(2a) + u_{A-A}(4a) + \dots \} \\
 &= N \left\{ \sum_{n=1}^{N/2} {}'u_{A-B}(na) + \sum_{n=2}^{N/2} {}'u_{A-A}(na) \right\}
 \end{aligned} \tag{32}$$

where \sum' denotes the summation with step $\Delta n = 2$ and subscripts $A-A$ and $A-B$ denote the interactions between atoms belonging to the same specie and different species, respectively. Similar to Eq.(27b), the equilibrium atomic spacing of the compound chain a_0 can be obtained by the minimization of the total energy as

$$-u'_{A-B}(a_0) = \sum_{n=2}^{N/2} {}'nu'_{A-A}(na_0) + \sum_{n=3}^{N/2} {}'nu'_{A-B}(na_0) \tag{33}$$

Fig. 15. One-side force acting on Zn-atom i .Fig. 16. Terms in the summations of Eq.(29) for force: (a) f_O ; (b) f_{Zn} .

According to the parameters in Buckingham potentials of ZnO, the equilibrium lattice constant a_0 governed by Eq.(33) is 1.653 Å.

Now, we can turn to the one-side force f_A acting on an atom belonging to specie A in the binary compound chain, as shown in Fig.15. Similar to the derivation of Eq.(29), the one-side force acting on the atom f_A in the binary compound chain can be derived as

$$\mathbf{f}_A = \left[\sum_{n=2}^{N/2} (n-1) u'_{A-A}(na_0) + \sum_{n=3}^{N/2} (n-1) u'_{A-B}(na_0) \right] \mathbf{e}_r \quad (34)$$

According to Eq.(34), the one-side forces f_O and f_{Zn} acting on O-atom and Zn-atom are calculated. All terms in the summations of Eq.(34) for both forces f_O and f_{Zn} are plotted in Fig.16. Although there are some oscillations in the plots, the summations are definitely negative, because of the predominate negative term $u'_{A-A}(2a_0)$ resulting from the long range Coulomb repulsive interactions (i.e. black dots in Fig.16). Above all, the two one side forces f_O and f_{Zn} are -2.730 eV/Å and -2.697 eV/Å , respectively, and are attractive as anticipated in §2.2.

Because of the attractive one-side force acting on the atom in the bulk ZnO, the atom near the free surface would shrink inwards, not always tends to expand outwards as claimed by Leach^[9] and Trimble^[19], once a free surface is created. To illustrate this issue, the spacing of a semi-infinite one-dimensional ZnO chain is calculated accordingly and the results are shown in Fig.17. It can be seen from Fig.17 that the outermost spacing becomes less than that in the bulk and the general tendency of the spacing variation near the surface is also shrinking, although some oscillations appear near the surface. The average spacing of the first twenty atoms near the surface is 1.649 Å, a bit less than that in the bulk 1.653 Å. As a result, the surface layer could be stiffer and the corresponding elastic modulus would increase with the decreasing sample size, e.g. the length of the chain. We calculate the modulus of the one-dimensional ZnO chain, defined as the ratio of the force to the strain, to check if the above supposition is valid, namely the modulus would increase with decreasing sample size. The linear fitting of the force-strain curves for 5-atom, 7-atom and infinite one-dimensional ZnO chain are shown in Fig.18. It can be seen from Fig.18 that the modulus increases with the decreasing size. These results justify the inverse size dependence of ZnO. Actually, this sort of inverse size dependence of increasing modulus with decreasing sample size has been obtained by means of molecular dynamics (MD) as well as molecular statistical thermodynamics (MST) simulations of ZnO nanorods^[7,8,20]. So, the multi-fold cross check clearly validates the inverse size dependence of elastic modulus in ZnO with Buckingham potential including long range Coulomb interaction.

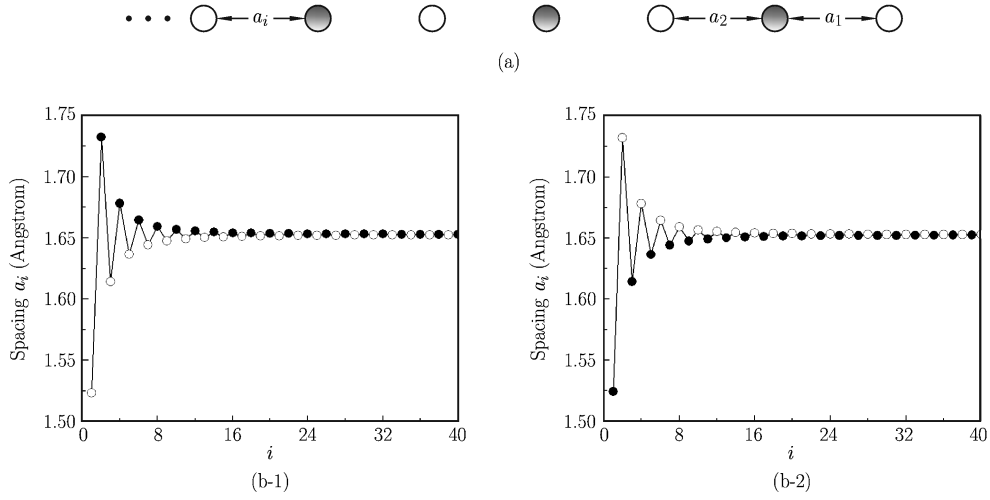


Fig. 17. A semi-infinite one-dimensional ZnO chain (a) and its atomic spacing (b). (b-1) the outmost atom is O-atom; (b-2) the outmost atom is Zn-atom.

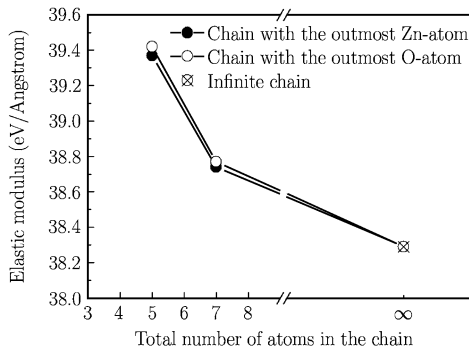


Fig. 18. Elastic moduli as functions of the total number of atoms.

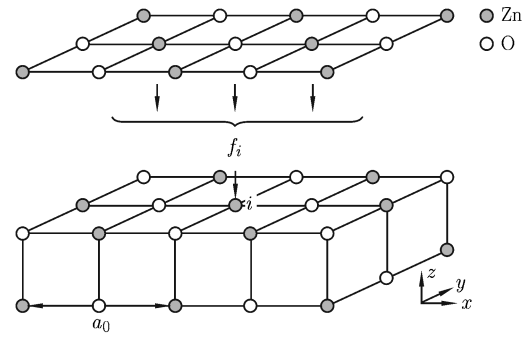


Fig. 19. Schematic diagram of one-side force exerted on atom i from all unilateral atoms above.

As an practical example, the lattice constant a_0 of infinite rocksalt ZnO lattice and the corresponding one-side force exerting on a representative atom i from all unilateral atoms (for instance all atoms above atom i , as shown in Fig.19) are also calculated as $a_0 = 4.849 \text{ \AA}$, and the one-side force f_O and f_{Zn} are equal to -1.249 eV/\AA and -1.160 eV/\AA respectively, which are once again attractive forces as shown in the one dimensional chain.

V. SURFACE EFFECT ON ELASTIC MODULUS DUE TO MANY-BODY FINNIS-SINCLAIR POTENTIAL

In this section, we examine a kind of many-body potential, namely Finnis-Sinclair potential for Cu to study the influence of many-body effect on the surface layer and size effects. The form of this potential is written as

$$\begin{aligned}
 U &= \sum_i u_i, \quad u_i = -\sqrt{\rho_i} + \frac{1}{2} \sum_{j \neq i} V_{ij}, \quad \rho_i = \sum_{j \neq i} \phi_{ij} \\
 V_{ij} &= \sum_{k=1}^6 a_k (r_k - r_{ij})^3 H(r_k - r_{ij}) \\
 \phi_{ij} &= \sum_{k=1}^2 A_k (R_k - r_{ij})^3 H(R_k - r_{ij}) \\
 H(x) &= \begin{cases} 0 & (x < 0) \\ 1 & (x > 0) \end{cases}
 \end{aligned} \tag{35}$$

where U is the total potential of system; u_i the potential of atom i ; ρ_i electron density; V_{ij} is the pair potential; a_k, r_k, A_k and R_k are potential parameters. The profiles of these many-body and pair potentials for Cu^[21] are shown in Fig.20, the pair potential is repulsive while many-body potential is attractive.

Similar to Eq.(25) and Eq. (27b), the total potential energy and equilibrium atomic spacing a_0 of an infinite chain can be obtained. After separating this infinite chain into two semi-infinite chains, we can also calculate one-side force exerting on the outmost atom i from all other atoms of the semi-infinite chain. According to the parameters in Finnis-Sinclair potentials of Cu, one-side force f_i is equal to $-0.4263 \text{ eV}/\text{\AA}$, which is an attractive one-side force. This involves two contributions from pair potential ($-0.004788 \text{ eV}/\text{\AA}$) as well as many-body potential ($-0.4215 \text{ eV}/\text{\AA}$). For the case of an infinite uniform fcc lattice being separated into two semi-infinite bodies by a (001) plane, the one-side force is also calculated and is $-0.9770 \text{ eV}/\text{\AA}$, also an attractive force. Consequently, the lattice near the free surface for a fcc lattice with many-body Finnis-Sinclair potential would be tighter than the bulk and result in increasing modulus with decreasing size.

To justify this size effect, the elastic moduli E in $\langle 100 \rangle$ direction of FCC Cu nanofilms with different thicknesses are numerically calculated using molecular statics (MS), see Fig.21. As anticipated, the elastic modulus does increase with the decreasing thickness.

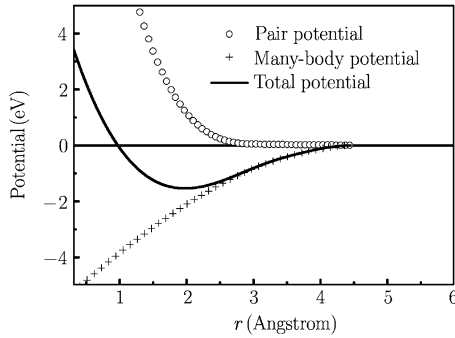


Fig. 20. Profiles of pair potential, many-body potential and total potential between two atoms.

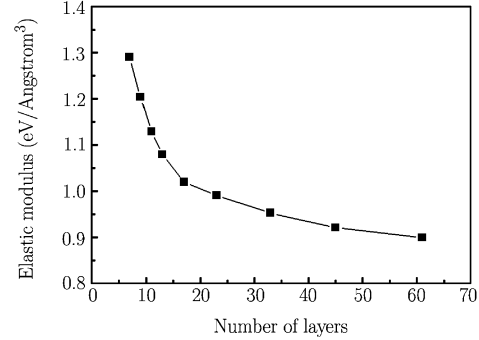


Fig. 21. Elastic moduli in $\langle 100 \rangle$ direction as functions of number of layers.

VI. CONCLUSIONS

In this paper, we firstly analyzed the surface microstructure and the surface effect on elastic moduli of a fcc nanofilm with (001) surface based on Lennard-Jones potential. It is found that the lattice near the surface is no longer uniform but becomes looser than that in the bulk and the elastic modulus in $\langle 100 \rangle$ direction decreases with decreasing thickness. This agrees well with previous numerical results^[6]. It is worthy noting that the decrease in elastic modulus should be attributed to the looseness of the surface layer as well as the smaller coordination number.

More importantly, it is found with one dimensional model that the looseness of the surface layer results from the surplus of the force $-u'(a)$ due to the nearest atom ($n = 1$) to all other long range interactions ($\sum u'(na), n \geq 2$) in a pair potential. In particular, the surplus can be uniquely expressed by a certain summation of the long range interactions ($\sum (n-1)u'(na), n \geq 2$) in pair potential. Hence, the lattice near the surface is not always loose as stated by Leach^[9] but can become either looser or tighter than that in the bulk depending on the sign of the sum.

As an example of the inverse size effect, Buckingham potential with long range Coulomb interaction in ZnO is examined. Rather than the looser lattice near the surface for the materials with Lennard-Jones potential, the atomic lattice near the surface in ZnO becomes tighter than that in the bulk. This can also be explained by the surplus of the nearest force to the long range interactions ($n \geq 2$) in the pair potential. Actually, the tightened lattice near the surface in ZnO results from the long range Coulomb interaction. In addition, the elastic modulus of one-dimensional ZnO chain shows increasing modulus with decreasing size.

For many-body Finnis-Sinclair potential, there is not such a concise expression of the one-side force, but still the long range repulsive interaction along with the electron redistribution effect leads to the tighter surface layer and the increasing modulus with decreasing size.

In conclusion, the difference in atomic/molecular pair potentials, especially their long-range interactions (attractive or repulsive) results in two kinds of surface layer (looser or tighter surface layer) and leads to two kinds of size dependence of elastic moduli in nano-scale materials (decreased or increased modulus with decreasing size). For many-body potential, the long-range interactions along with the many-body effect lead to microstructural variations near the surface and size effects of elastic modulus. Generally speaking, the size effect of materials could be attributed to the microstructure near surface, governed by the corresponding atomic/molecular potentials. After using the symbol \Leftarrow to represent the governing relationship, the dominated mechanisms governing the two kinds of size effects can be qualitatively summarized in Table 3.

Table 3. Summary of the dominated mechanisms governing the two kinds of size effects

Elastic modulus decreases with decreasing size	Elastic modulus increases with decreasing size
\uparrow	\uparrow
Looser atomic lattice near surface than the bulk	Tighter atomic lattice near surface than the bulk
\uparrow	\uparrow
The atom in the bulk is in the balance of repulsive one-side forces	The atom in the bulk is in the balance of attractive one-side forces
\uparrow	\uparrow
Long range attractive interactions in pair potentials, $(\sum (n-1)u'(na) > 0, n \geq 2)$ (like Mie-type potentials)	Long range repulsive interactions in pair potentials, $(\sum (n-1)u'(na) < 0, n \geq 2)$ (like Coulomb interaction)

References

- [1] Li, X.X., Ono, T., Wang, Y.L. and Esashi, M., Ultrathin single-crystalline-silicon cantilever resonators: Fabrication technology and significant specimen size effect on Young's modulus. *Applied Physics Letters*, 2003, 83(15): 3081-3083.
- [2] Cuenot, S., Fretigny, C., Demoustier-Champagne, S. and Nysten, B., Surface tension effect on the mechanical properties of nanomaterials measured by atomic force microscopy. *Physical Review B*, 2004, 69(16): 165410.
- [3] Chen, C.Q., Shi, Y., Zhang, Y.S., Zhu, J. and Yan, Y.J., Size Dependence of Young's Modulus in ZnO Nanowires. *Physical Review Letters*, 2006, 96(7): 075505.
- [4] Agrawal, R., Peng, B., Gdoutos, E.E. and Espinosa, H.D., Elasticity Size Effects in ZnO Nanowires-A Combined Experimental-Computational Approach. *Nano Letters*, 2008, 8(11): 3668-3674.
- [5] Streitz, F.H., Sieradzki, K. and Cammarata, R.C., Elastic properties of thin fcc films. *Physical Review B, Rapid Communications*, 1990, 41(7): 12285-12287.
- [6] Zhou, L.G. and Huang, H.C., Are surfaces elastically softer or stiffer? *Applied Physics Letters*, 2004, 84(11): 1940-1942.
- [7] Kulkarni, A.J., Zhou, M. and Ke, F.J., Orientation and size dependence of the elastic properties of zinc oxide nanobelts. *Nanotechnology*, 2005, 16(12): 2749-2756.
- [8] Hu, J. and Pan, B.C., Surface effect on the size- and orientation-dependent elastic properties of single-crystal ZnO nanostructures. *Journal of Applied Physics*, 2009, 105(3): 034302.
- [9] Gurtin, M.E. and Murdoch, A.I., A continuum theory of elastic material surfaces. *Archives for Rational Mechanics and Analysis*, 1975, 57(4): 291-323.
- [10] Streitz, F.H., Cammarata, R.C. and Sieradzki, K., Surface-stress effects on elastic properties. I. Thin metal films. *Physical Review B*, 1994, 49(15): 10699-10706.
- [11] Sharma, P., Ganti, S. and Bhate, N., Effect of surfaces on the size-dependent elastic state of nano-inhomogeneities. *Applied Physics Letters*, 2003, 82(4): 535-537.
- [12] Zhang, T.Y., Luo, M. and Chan, W.K., Size-dependent surface stress, surface stiffness, and Young's modulus of hexagonal prism [111] β -SiC nanowires. *Journal of Applied Physics*, 2008, 103(10): 104308.
- [13] Miller, R.E. and Shenoy, V.B., Size-dependent elastic properties of nanosized structural elements. *Nanotechnology*, 2000, 11(3): 139-147.
- [14] Krivtsov, A.M. and Morozov, N.F., On Mechanical Characteristics of Nanocrystals. *Physics of the Solid State*, 2002, 44(1): 2260-2265.

- [15] Sun,C.T. and Zhang,H.T., Size-dependent elastic moduli of plate like nanomaterials. *Journal of Applied Physics*, 2003, 93(2): 1212-1218.
- [16] Chang,I.L., Chang,S.H. and Huang,J.C., The theoretical model of fcc ultrathin film. *International Journal of Solids and Structures*, 2007, 44(18-19): 5818-5828.
- [17] Leach, Andrew R., Molecular Modelling: Principles and Applications. Prentice Hall, 2001: 241.
- [18] Kittel,C., Introduction to Solid State Physics. 5th ed. New York: Wiley, 1976: 65.
- [19] Trimble,T.M. and Cammarata,R.C., Many-body effects on surface stress, surface energy and surface relaxation of fcc metals. *Surface Science*, 2008, 602(14): 2339.
- [20] Xiao,P., Wang,J., Ke,F.J., Xia,M.F. and Bai,Y.L., Application of molecular statistical thermodynamics to uniaxial tension of ZnO nanorods. In: XXII International Congress of Theoretical and Applied Mechanics, Abstract Book, 2008: 298.
- [21] Ackland,G.J. and Vitek,V., Many-body potentials and atomic-scale relaxations in noble-metal alloys. *Physical Review B*, 1990, 41(15): 10324-10333.